Monthly Notices of the ROYAL ASTRONOMICAL SOCIETY

MNRAS **446,** 2560–2565 (2015) doi:10.1093/mnras/stu2253

Limits on low-frequency radio emission from southern exoplanets with the Murchison Widefield Array

Tara Murphy,[1,2★] Martin E. Bell,[1,2,3] David L. Kaplan,[4] B. M. Gaensler,[1,2] André R. Offringa,[2,5] Emil Lenc,[1,2] Natasha Hurley-Walker,[6] G. Bernardi,[7,8,9] J. D. Bowman,[10] F. Briggs,[2,5] R. J. Cappallo,[11] B. E. Corey,[11] A. A. Deshpande,[12] D. Emrich,[6] R. Goeke,[13] L. J. Greenhill,[7] B. J. Hazelton,[14] J. N. Hewitt,[13] M. Johnston-Hollitt,[15] J. C. Kasper,[7,16] E. Kratzenberg,[11] C. J. Lonsdale,[11] M. J. Lynch,[6] S. R. McWhirter,[11] D. A. Mitchell,[2,3] M. F. Morales,[14] E. Morgan,[13] D. Oberoi,[17] S. M. Ord,[2,6] T. Prabu,[12] A. E. E. Rogers,[11] D. A. Roshi,[18] N. Udaya Shankar,[12] K. S. Srivani,[12] R. Subrahmanyan,[2,12] S. J. Tingay,[2,6] M. Waterson,[5,6] R. B. Wayth,[2,6] R. L. Webster,[2,19] A. R. Whitney,[11] A. Williams[6] and C. L. Williams[13]

[1]*Sydney Institute for Astronomy, School of Physics, The University of Sydney, NSW 2006, Australia*
[2]*ARC Centre of Excellence for All-sky Astrophysics (CAASTRO)*
[3]*CSIRO Astronomy and Space Science, Marsfield, NSW 2122, Australia*
[4]*Department of Physics, University of Wisconsin–Milwaukee, Milwaukee, WI 53201, USA*
[5]*Research School of Astronomy and Astrophysics, Australian National University, Canberra, ACT 2611, Australia*
[6]*International Centre for Radio Astronomy Research, Curtin University, Bentley, WA 6102, Australia*
[7]*Harvard–Smithsonian Center for Astrophysics, Cambridge, MA 02138, USA*
[8]*SKA SA, 3rd Floor, The Park, Park Road, Pinelands 7405, Cape Town, South Africa*
[9]*Department of Physics and Electronics, Rhodes University, Grahamstown, 6140, South Africa*
[10]*School of Earth and Space Exploration, Arizona State University, Tempe, AZ 85287, USA*
[11]*MIT Haystack Observatory, Westford, MA 01886, USA*
[12]*Raman Research Institute, Bangalore 560080, India*
[13]*Kavli Institute for Astrophysics and Space Research, Massachusetts Institute of Technology, Cambridge, MA 02139, USA*
[14]*Department of Physics, University of Washington, Seattle, WA 98195, USA*
[15]*School of Chemical & Physical Sciences, Victoria University of Wellington, Wellington 6140, New Zealand*
[16]*Department of Atmospheric, Oceanic and Space Sciences, University of Michigan, Ann Arbor, MI 48109, USA*
[17]*National Centre for Radio Astrophysics, Tata Institute for Fundamental Research, Pune 411007, India*
[18]*National Radio Astronomy Observatory, Charlottesville and Greenbank, Charlottesville, VA 22903-2475, USA*
[19]*School of Physics, The University of Melbourne, Parkville, VIC 3010, Australia*

Accepted 2014 October 23. Received 2014 October 22; in original form 2014 September 11

ABSTRACT

We present the results of a survey for low-frequency radio emission from 17 known exoplanetary systems with the Murchison Widefield Array. This sample includes 13 systems that have not previously been targeted with radio observations. We detected no radio emission at 154 MHz, and put 3σ upper limits in the range 15.2–112.5 mJy on this emission. We also searched for circularly polarized emission and made no detections, obtaining 3σ upper limits in the range 3.4–49.9 mJy. These are comparable with the best low-frequency radio limits in the existing literature and translate to luminosity limits of between 1.2×10^{14} and 1.4×10^{17} W if the emission is assumed to be 100 per cent circularly polarized. These are the first results from a larger program to systematically search for exoplanetary emission with the MWA.

Key words: radio continuum: planetary systems.

1 INTRODUCTION

Magnetized extrasolar planets are expected to emit strongly at radio wavelengths, in the same way as magnetized planets in our own

★E-mail: tara@physics.usyd.edu.au

Solar system (Winglee, Dulk & Bastian 1986; Zarka et al. 2001). Intense emission can be generated by the electron–cyclotron maser instability if the planet has an intrinsic magnetic field and a source of energetic electrons (Dulk 1985). This emission is sporadic, with variability time-scales spanning seconds to days. Unlike in the optical regime, in which radiation from planets is much weaker than that of their parent star, in radio it can be of comparable strength: Jupiter's radio emission in the decametre band is as intense as solar radio bursts (Zarka et al. 2001). The strongest exoplanetary emission is likely to be from planets that are more massive than Jupiter, orbiting their parent star at short orbital distances.

A majority of exoplanets have been discovered through indirect means such as radial velocity and transit searches (Perryman 2011). A small number of known exoplanets[1] have been detected through direct imaging, and radio observations provide another method of making direct detections. Radio observations of exoplanets would allow us to confirm that the planet has a magnetic field, and put a limit on the magnetic field strength near the surface of the planet (Hess & Zarka 2011). The detection of circular polarization would indicate which magnetic hemisphere the emission comes from and would give a limit on the plasma density in the magnetosphere (Bastian, Dulk & Leblanc 2000).

Early attempts to detect radio emission from exoplanets occurred before the discovery of the first exoplanet around a main sequence star, 51 Peg, by Mayor & Queloz (1995). For example, Winglee et al. (1986) targeted six nearby stars with the Very Large Array (VLA) at 333 and 1400 MHz, but made no detections. More recently, there have been a number of attempts to detect radio emission from known exoplanets. Bastian et al. (2000) conducted a search of seven exoplanets with the VLA at 333 and 1465 MHz and one at 74 MHz. They made no detections, with typical 3σ upper limits of 0.06–0.21 mJy at 1465 MHz, 3–30 mJy at 333 MHz and 150 mJy at 74 MHz. Lazio et al. (2004) observed five exoplanets with the VLA at 74 MHz, as part of the VLA Low Frequency Sky Survey, finding 3σ upper limits of 262–390 mJy. George & Stevens (2007) targeted ϵ Eri and HD 128311 at 150 MHz with the Giant Metrewave Radio Telescope (GMRT). They reported 3σ limits of 9.4 and 18.6 mJy, respectively, for the two systems. Smith et al. (2009) targeted HD 189733 during the planet's secondary eclipse, reporting a 3σ upper limit of 81 mJy in the frequency range 307–347 MHz. Lazio et al. (2010) targeted HD 80606b with the VLA and reported 3σ limits of 1.7 mJy at 325 MHz and 48 μJy at 1425 MHz. Stroe, Snellen & Röttgering (2012) observed τ Bootis at 1.7 GHz with the Westerbork Synthesis Radio Telescope, and reported a 3σ upper limit of 0.13 mJy on emission from the exoplanetary system. Hallinan et al. (2013) observed τ Bootis with the GMRT, reporting a 3σ upper limit of 1.2 mJy at 150 MHz.

GMRT observations of the Neptune-mass exoplanet HAT-P-11b by Lecavelier des Etangs et al. (2013) show a possible detection of radio emission. If the emission is associated with the planet, then the flux density is 3.87 mJy at 150 MHz. However, they reported that the detection was not confirmed in follow-up observations, and deeper observations are required. The largest radio survey of exoplanets to date was conducted by Sirothia et al. (2014), with data from the TIFR GMRT Sky Survey. No detections were made, with 150 MHz 3σ upper limits of between 8.7 and 136 mJy placed on 171 planetary systems. In summary, there have been no confirmed detections of planetary systems at radio wavelengths to date.

[1] See http://exoplanet.eu/catalog for a complete catalogue (Schneider et al. 2011).

Cyclotron maser emission has a maximum frequency determined by the electron gyrofrequency and is proportional to the magnetic field strength (see equation 1; Farrell, Desch & Zarka 1999). Cyclotron maser emission is 100 per cent circularly polarized, and so planets should be detectable in circular polarization (Stokes *V*) at similar levels to their total intensity (Stokes *I*) emission. Exoplanetary radio emission is expected to peak at frequencies less than 10–100 MHz (see for example, Grießmeier, Zarka & Spreeuw 2007) and hence has been inaccessible by most telescopes.

In this paper, we present a search for low-frequency radio emission from known exoplanets with the Murchison Widefield Array (MWA; Lonsdale et al. 2009; Bowman et al. 2013; Tingay et al. 2013). We have targeted 17 exoplanetary systems that fall within the region of the MWA Transients Survey (MWATS), a blind survey for transients and variables. The MWA sensitivity is confusion limited in Stokes *I*. However, we take advantage of the low density of circularly polarized sources and hence the improved sensitivity in Stokes *V* to conduct deeper searches for polarized radio emission from these sources. Using the assumption that the circularly polarized emission is a large fraction of the total intensity, these limits can be used to calculate luminosity limits. Note that this also ignores the likely time variability of exoplanetary radio emission.

2 OBSERVATIONS AND DATA ANALYSIS

The Murchison Widefield Array is a 128-tile low-frequency radio interferometer located in Western Australia. It operates between 80 and 300 MHz with a processed bandwidth of 30.72 MHz for both linear polarizations. The 128 tiles are distributed over an ∼3-km diameter area, with a minimum baseline of 7.7 m and a maximum baseline of 2864 m. MWA operations began in 2013 June. See Hurley-Walker et al. (2014) and Bell et al. (2014) for a description of the MWA observing modes.

We obtained observations between 2013-07-09 and 2014-06-13 (UTC) as part of the MWATS survey (Bell et al., in preparation). Three different meridian declination strips at Dec $=1\overset{\circ}{.}6$, $-26\overset{\circ}{.}7$ (zenith) and -55° were observed in drift scan mode for a whole night, at a cadence of approximately once per month (at 154 MHz). Each declination was observed in turn with an integration time of 2 min. The ∼25° field of view (equivalent to about 2 h of sidereal time) means that each observation overlaps with the previous one at the same declination. The specific declination strips that contained our target sources for this work are summarized in Table 1.

Table 1. Observations used in this paper. The name of each epoch consists of the month of observation and the declination strip observed. *N* gives the number of individual snapshot observations taken that night.

Epoch	Start Date (UTC)	End Date (UTC)	*N*
Sep −55°	2013-09-16 13:30:39	2013-09-16 21:24:39	77
Dec −55°	2013-12-06 13:53:27	2013-12-06 20:05:27	60
Dec $+1\overset{\circ}{.}6$	2013-12-06 13:51:27	2013-12-06 20:09:27	61
Apr $+1\overset{\circ}{.}6$	2014-04-28 10:51:59	2014-04-28 20:45:59	96
Apr −26°	2014-04-28 10:49:59	2014-04-28 20:43:51	96
Apr −55°	2014-04-28 10:47:59	2014-04-28 20:41:59	96
Jun −26°	2014-06-09 11:16:15	2014-06-09 20:56:15	55
Jun −55°	2014-06-12 11:04:31	2014-06-13 20:20:23	74

Table 2. Properties of exoplanetary systems targeted in our survey. N_p is the number of known planets in the system. Where there are multiple planets, the properties are given for the first discovered planet (which in all cases except Gliese 876 b is the planet closest to its host star). a is the semimajor axis and D is the distance to the star. S_{150} is best low-frequency (150 MHz) 3σ flux limit from the literature where available (Geo07: George & Stevens 2007) and (Sir14: Sirothia et al. 2014). Note that Sirothia et al. (2014) report a 120 mJy source at 3.2 arcsec from the position of 61 Vir. However, it is likely this is a background source unassociated with the exoplanetary system (see the text for more details).

Name	RA (J2000)	Dec (J2000)	Discovery year	D (pc)	N_p	Mass (M_J)	Period (d)	a (au)	S_{150} (mJy)	Reference
WASP-18 b	01:37:25	−45:40:40	2009	100.0	1	10.43	0.9	0.02		
Gl 86 b	02:10:25	−50:49:25	2000	10.9	1	4.01	15.8	0.11		
ϵ Eri b	03:32:55	−09:27:29	2000	3.2	2	1.55	2502.0	3.39	<9.36	Geo07
HD 37605 b	05:40:01	+06:03:38	2004	44.0	2	2.81	55.0	0.28		
HD 41004 B b	05:59:49	−48:14:22	2004	43.0	1	18.40	1.3	0.02		
HD 102365 b	11:46:31	−40:30:01	2011	9.2	1	0.05	122.1	0.46		
61 Vir b	13:18:23	−18:18:39	2009	8.5	3	0.02	4.2	0.05		
HD 128311 b	14:36:00	+09:44:47	2002	16.6	2	2.18	448.6	1.10	<18.60	Geo07
HIP 79431 b	16:12:41	−18:52:32	2010	14.4	1	2.10	111.7	0.36	<11.40	Sir14
HD 147018 b	16:23:00	−61:41:20	2009	43.0	2	2.12	44.2	0.24		
HD 147513 b	16:24:01	−39:11:34	2003	12.9	1	1.21	528.4	1.32		
GJ 674 b	17:28:40	−46:53:43	2007	4.5	1	0.04	4.7	0.04		
HD 162020 b	17:50:37	−40:19:05	2002	31.3	1	14.40	8.4	0.07		
HD 168443 b	18:20:04	−09:35:34	1998	37.4	2	7.66	58.1	0.29		
Gl 785 b	20:15:16	−27:01:59	2010	8.9	1	0.05	74.7	0.32	<14.70	Sir14
GJ 832 b	21:33:34	−49:00:32	2008	4.9	1	0.64	3416.0	3.40		
Gliese 876 b	22:53:13	−14:15:12	2000	4.7	4	1.93	61.0	0.21		

2.1 Data reduction

Our data reduction and analysis procedure follows the approach described by Bell et al. (2014). Each declination strip was calibrated using a two minute observation of a bright, well-modelled source. A single time-independent, frequency dependent amplitude and phase calibration solution was applied to all observations for a given night (per declination strip). For each snapshot observation, the visibilities were preprocessed with the COTTER MWA preprocessing pipeline, which flags radio-frequency interference using the AOFLAGGER (Offringa, van de Gronde & Roerdink 2012), averages the data and converts the data to the CASA measurement set format. The observations were then imaged and cleaned using the WSCLEAN algorithm (Offringa et al. 2014). A pixel size of 0.75 arcsec and image size of 3072 pixels was used for imaging.

The WSCLEAN algorithm was used to produce both Stokes I images with Briggs weighting −1 (closer to uniform weighting) and Stokes V images with Briggs weighting +1 (closer to natural weighting). The WSCLEAN algorithm does this by forming a 2×2 complex Jones matrix $\mathbf{I}$ for each image pixel. Beam correction is then applied by inverting the beam voltage matrix $\mathbf{B}$, and computing $\mathbf{B}^{-1}\mathbf{I}\mathbf{B}^{*-1}$ where $*$ denotes the conjugate transpose. A full description of this approach is given by Offringa et al. (2014). Note that some aspects of the MWA data reduction process are being improved, and so future work is likely to have somewhat better sensitivity than presented here.

For each of the declination strips the resulting images (in Stokes I and Stokes V) were mosaicked together (co-added and weighted by the primary beam) to increase the sensitivity, as described by Hurley-Walker et al. (2014). Our final data product consisted of a series of snapshot images with two minute integrations, and a mosaicked image that combined all the snapshot images for a single night of observing (the number of snapshots in each night is given in Table 1).

2.2 Sample selection

Of the 1110 confirmed exoplanetary systems,[2] 347 fall within the region covered by the MWATS survey as at 2014 June. We calculated the expected maximum emission frequency and flux density using the models of Lazio et al. (2004) and selected the sources for which these parameters were close to or above the MWA detection capabilities. We also included the sources listed by Nichols (2012) as the 10 most likely candidates for radio emission generated by magnetosphere–ionosphere coupling. This resulted in a sample of 17 of the most likely candidates for detectable emission at MWA frequencies. 15 of these sources are in the Southern hemisphere and, as most previous studies have focused on northern samples, have not previously been targeted with radio observations. Table 2 lists the key properties of the exoplanetary systems in our sample.

3 RESULTS AND DISCUSSION

We searched the individual snapshot images and mosaicked images in Stokes I and Stokes V for all of the exoplanetary systems in our sample. No radio sources were detected at the positions of any of the systems considered, within the MWA position errors. For each source, we measured the upper limit on the Stokes I and Stokes V emission in each snapshot image and in the mosaicked image by calculating the rms in a box several times the synthesized beam, centred on the source position. Table 3 shows the best-measured limits from the mosaicked images (effectively limits on steady emission from these systems). Each target source typically appeared in ∼20–30 snapshot images, so the limits in the snapshot images (which have an integration time of 2 min and a cadence of 6 min) were typically a factor of ∼4–6 times higher than the mosaicked images.

[2] From the exoplanet.eu catalogue, as of 2014 May 14.

Table 3. Our measured 3σ flux density S_{154} upper limits and derived luminosity L limits for Stokes I total intensity emission and Stokes V circularly polarized emission, and comparison to theoretical predictions from the literature.

Name	MWA 154 MHz				Lazio et al. (2004)		Grießmeier et al. (2011)		Nichols (2012)	
	S_{154} (I) (mJy)	L (I) (W)	S_{154} (V) (mJy)	L (V) (W)	ν_c (MHz)	S_ν (mJy)	ν_c (MHz)	S_ν (mJy)	$S_{1,24}$ (mJy)	$S_{3,54}$ (mJy)
WASP-18	<15.2	$<2.2 \times 10^{17}$	<3.4	$<5.1 \times 10^{16}$	812	6.8	92	50	–	–
Gl 86	<16.4	$<2.9 \times 10^{15}$	<4.6	$<8.1 \times 10^{14}$	464	36.7	61	4	0.05	1.57
ϵ Eridani	<51.0	$<7.7 \times 10^{14}$	<7.7	$<1.2 \times 10^{14}$	95	2.4	33	20	0.61	18.21
HD 37605	<93.0	$<2.6 \times 10^{17}$	<10.9	$<3.1 \times 10^{16}$	257	0.6	49	2	–	–
HD 41004 B	<68.6	$<1.9 \times 10^{17}$	<14.5	$<4.0 \times 10^{16}$	1832	33.5	172	600	–	–
HD 102365	<45.3	$<5.7 \times 10^{15}$	<9.0	$<1.1 \times 10^{15}$	<1	22.7	3	0	0.07	2.17
61 Vir	–	–	<6.6	$<7.0 \times 10^{14}$	<1.0	2206.0	–	–	0.08	2.55
HD 128311	<43.7	$<1.8 \times 10^{16}$	<10.0	$<4.0 \times 10^{15}$	168	0.5	41	1	–	–
HIP 79431	<50.0	$<1.5 \times 10^{16}$	<13.7	$<4.2 \times 10^{15}$	158	3.9	40	0	–	–
HD 147018	<76.3	$<2.1 \times 10^{17}$	<49.9	$<1.4 \times 10^{17}$	160	0.8	40	0	–	–
HD 147513	<73.1	$<1.8 \times 10^{16}$	<24.2	$<5.9 \times 10^{15}$	63	0.7	27	2	–	–
GJ 674	<42.4	$<1.3 \times 10^{15}$	<14.6	$<4.4 \times 10^{14}$	<1	8975.5	1	5000	0.30	9.04
HD 162020	<85.6	$<1.2 \times 10^{17}$	<27.4	$<3.9 \times 10^{16}$	191	10.3	145	8	–	–
HD 168443	<112.5	$<2.3 \times 10^{17}$	<33.2	$<6.8 \times 10^{16}$	1365	0.5	97	0	–	–
Gl 785	<38.7	$<4.5 \times 10^{15}$	<11.2	$<1.3 \times 10^{15}$	<1	42.7	4	0	0.08	2.39
GJ 832	<16.8	$<6.0 \times 10^{14}$	<4.7	$<1.7 \times 10^{14}$	21	1.4	18	0	0.25	7.59
Gliese 876	<66.3	$<2.1 \times 10^{15}$	<17.3	$<5.6 \times 10^{14}$	136	91.0	42	6	0.28	8.38

Note that an imperfect MWA primary beam model means that flux density measurements far from the phase centre of an observation could have errors of up to 10 per cent (Hurley-Walker et al. 2014). The polarization leakage has been estimated empirically by measuring the polarization of bright sources as they pass through the primary beam. The leakage is typically 1–2 per cent at zenith and up to 3–5 per cent at low elevations where the beam is less well modelled (Sutinjo et al., submitted).

We calculated luminosity limits from steady emission, assuming an emission bandwidth equal to the observing frequency (154 MHz) and a solid angle of 4π sr (i.e. we are ignoring any beaming of the emission). These are shown in columns 3 and 5 of Table 3 for Stokes I and Stokes V, respectively. For comparison, we have also converted the limits published in the literature using the same method. These are shown in Fig. 1, with our new limits as black circles.

The maximum emission frequency of cyclotron maser emission is at the electron gyrofrequency and is proportional to the maximum planetary magnetic field strength, B_p^{max} (Farrell et al. 1999):

$$f_c^{max} = \frac{e B_p^{max}}{2\pi m_e} = 2.8 B_p^{max}. \quad (1)$$

Hence a detection at 154 MHz would imply a magnetic field strength of $B_p = 55$ G.

The Jovian magnetic field, predicted by models based on spacecraft observations of Jupiter, ranges in strength from 2 to 14 G (Connerney 1993). Hence, for an exoplanet to be detected at 154 MHz, it would need a magnetic field strength approximately four times that of Jupiter's. Models of convection-driven dynamos in planets predict that young, giant extrasolar planets of 5–10 Jupiter masses could have a surface magnetic field strength 5–12 times larger than Jupiter's surface magnetic field (Christensen & Aubert 2006; Christensen, Holzwarth & Reiners 2009).

We have measured 3σ flux density limits between 3.4 and 49.9 mJy in Stokes V (see Table 3). The high values for several of the Stokes V limits are due to contamination from a nearby bright source or Galactic plane emission. Assuming 100 per cent circularly polarized emission, these translate to luminosity limits between 5.8×10^{13} and 6.8×10^{16} W. These are comparable to the best radio limits given in the literature for ϵ Eri (George & Stevens 2007) and 47 UMa (Bastian et al. 2000). Jupiter generates between 10^{10} and 10^{11} W of power between 1 and 40 MHz (Zarka, Cecconi & Kurth 2004), making our best limits about three orders of magnitude greater.

Table 3 also lists predicted radio flux densities from various models presented in the literature. Columns 6 and 7 give predictions for the characteristic emission frequency ν_c (in MHz) and the burst flux density at that frequency S_ν (in mJy) from Lazio et al. (2004). These are calculated from the radiometric Bode's law and Blackett's law (see Lazio et al. 2004), and then applying the assumption that burst flux density could be factor of 100 greater than these calculations. Our measured limits for Gl 86, GJ 674, 61 Vir, HD 41004 B, Gl 785 and Gliese 876 are lower than these predictions, although note that the characteristic emission frequency is predicted to be outside the MWA frequency range for all but two of these.

Grießmeier et al. (2007) and Grießmeier, Zarka & Girard (2011) present predictions based on three models of exoplanetary emission: a magnetic energy model, a kinetic energy model and a model in which exoplanets are assumed to be subject to frequent stellar eruptions similar to solar coronal mass ejections. Columns 8 and 9 of Table 3 gives the maximum predicted emission frequency ν (in MHz) and the corresponding flux density S_ν (in mJy) from these three models. For the three sources that have a predicted emission frequency within the range of the MWA (WASP-18, HD 41004 B and HD 162020) we provide constraining limits for the first two.

Finally, Nichols (2012) presents predictions based on a model of magnetosphere–ionosphere coupling in Jupiter-like exoplanets. Nichols (2012) gives predictions for the maximum flux density based on different values of dynamic pressure and planetary angular velocity. Column 10 gives the predicted flux density based on solar dynamic pressure and angular velocity (S_1, at 24 MHz, in mJy). Column 11 gives the predicted flux density based on solar dynamic pressure and 3 × solar angular velocity (S_3, at 54 MHz, in mJy). These predictions are all below our observed limits.

One of the sources in our target list, 61 Vir, was discussed by Sirothia et al. (2014), who reported a 120 mJy source at 150 MHz, located 3.2 arcsec from the position of the star. We detect a source

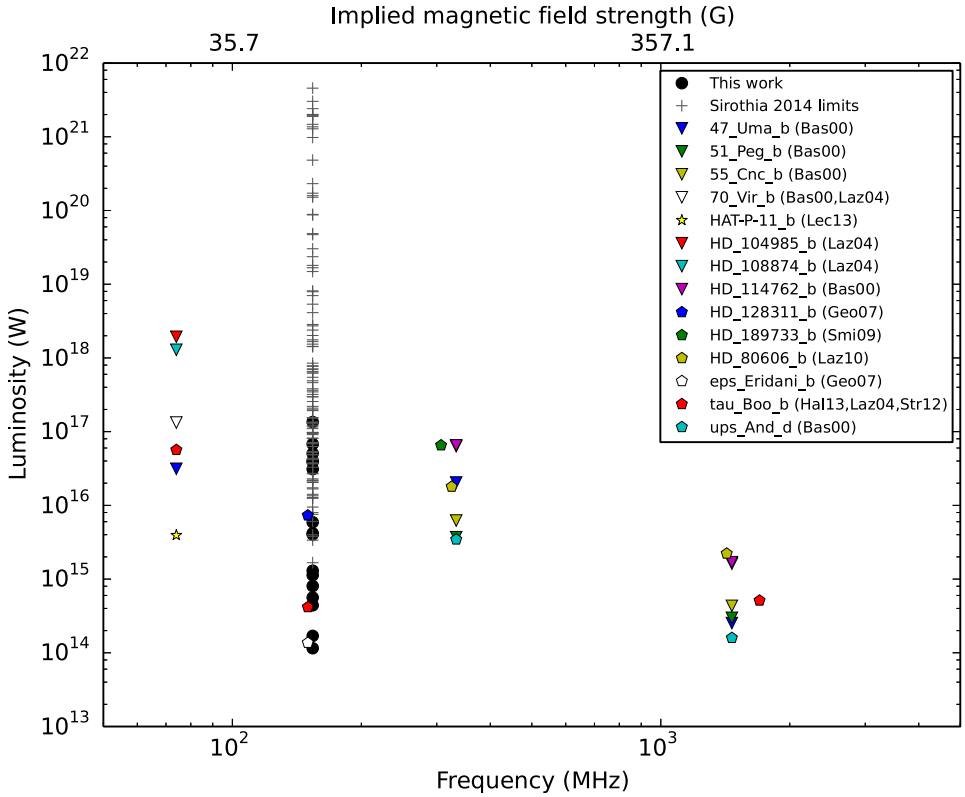

Figure 1. Luminosity limits on radio emission from exoplanets. The limits from this work, calculated from our Stokes *V* measurements, are shown as black circles. The references in the legend are: Bas00 (Bastian et al. 2000); Laz04 (Lazio et al. 2004); Geo07 (George & Stevens 2007); Smi09 (Smith et al. 2009); Laz10 (Lazio et al. 2010); Str12 (Stroe et al. 2012); Hal13 (Hallinan et al. 2013); Lec13 (Lecavelier des Etangs et al. 2013). The secondary *x*-axis gives the implied magnetic field strength $B_{\rm p}^{\rm max}$ calculated using equation (1).

at 187 mJy at the same position. This is an NVSS source (NVSS J131823-181851) with a flux density of 50.9 mJy at 1.4 GHz (Condon et al. 1998) and is also detected in the Westerbork In the Southern Hemisphere (WISH) survey with a flux density of 159 mJy at 325 MHz (De Breuck et al. 2002). The position of the source in NVSS, WISH and our MWA observations agree to within the respective survey errors. The high proper motion of 61 Vir ((1070.36, −1063.69) mas yr^{-1}; van Leeuwen 2007) argues against this radio source being associated with the star or planetary system. When the NVSS images were taken (between 1993 and 1996), the proper motion corrected position of 61 Vir would have been offset by at least 22.3 arcsec from the NVSS position, well outside the NVSS positional error of ∼1 arcsec. Hence we conclude that this is a background radio source that is not associated with 61 Vir.

4 CONCLUSION

We have presented the first results from a survey for low-frequency radio emission from 17 known exoplanets with the Murchison Widefield Array. This sample includes 13 exoplanets that have not previously been targeted with radio observations. We made no detections of radio emission at 154 MHz, and put upper limits in the range 15.2–112.5 mJy on this emission. We also searched for circularly polarized emission and made no detections, putting upper limits in the range 3.4–49.9 mJy. These are comparable with the best low-frequency radio limits in the existing literature and translate to luminosity limits in the range of 5.8×10^{13} to 6.8×10^{16} W if the emission is assumed to be 100 per cent circularly polarized.

As discussed by Bastian et al. (2000), there are a number of reasons which may explain why we have not made any detections. The most obvious is that we need more sensitive observations, as only our best limits place any constraints on predicted flux densities. The second issue is that our observing frequency, while lower than many previous observations of exoplanetary systems, is still too high compared to the predicted maximum emission frequency for many systems in our sample. These instrumental limitations will be reduced with future telescopes, and ultimately the Square Kilometre Array low-frequency instrument (Lazio et al. 2009).

In addition to these limitations, we need observations with better coverage of the planetary orbital period. Radio emission from exoplanetary systems is likely to be orbitally beamed, and so full coverage of a planetary orbital period would put a more stringent limit on the emission. Since we do not know the axis of beaming, it is critical to target a range of known exoplanets. As well as being modulated by the orbital frequency, it is likely that the emission is time variable. Hence the ideal observing program would involve constant monitoring of a large number of exoplanetary systems.

In future work with the MWA we will use lower frequency (90 MHz) observations and cover the full orbital period of several known systems to increase the probability of detection. There are also projects underway with LOFAR to search for exoplanetary radio emission (Zarka, Griessmeier & Tkp-ExoPlanets Working Group 2009). The development of the Square Kilometre Array low-frequency instrument (SKA1-Low) will provide an opportunity to detect exoplanets at low frequencies (a Jupiter-like planet could be detected out to ∼10 pc), and enable blind surveys which have the

potential to discover new exoplanetary systems through their radio emission Zarka, Lazio & Hallinan (in preparation).

ACKNOWLEDGEMENTS

We thank Elaine Sadler for useful discussions and Aina Musaeva for assistance with the data reduction. This scientific work makes use of the Murchison Radio-astronomy Observatory, operated by Commonwealth Scientific and Industrial Research Organisation (CSIRO). We acknowledge the Wajarri Yamatji people as the traditional owners of the Observatory site. Support for the MWA comes from the US National Science Foundation (grants AST-0457585, PHY-0835713, CAREER-0847753 and AST-0908884), the Australian Research Council (LIEF grants LE0775621 and LE0882938), the US Air Force Office of Scientific Research (grant FA9550-0510247) and the Centre for All-sky Astrophysics (an Australian Research Council Centre of Excellence funded by grant CE110001020). Support is also provided by the Smithsonian Astrophysical Observatory, the MIT School of Science, the Raman Research Institute, the Australian National University, and the Victoria University of Wellington (via grant MED-E1799 from the New Zealand Ministry of Economic Development and an IBM Shared University Research Grant). The Australian Federal government provides additional support via the CSIRO, National Collaborative Research Infrastructure Strategy, Education Investment Fund, and the Australia India Strategic Research Fund, and Astronomy Australia Limited, under contract to Curtin University. We acknowledge the iVEC Petabyte Data Store, the Initiative in Innovative Computing and the CUDA Center for Excellence sponsored by NVIDIA at Harvard University, and the International Centre for Radio Astronomy Research (ICRAR), a Joint Venture of Curtin University and The University of Western Australia, funded by the Western Australian State government.

REFERENCES

Bastian T. S., Dulk G. A., Leblanc Y., 2000, ApJ, 545, 1058
Bell M. E. et al., 2014, MNRAS, 438, 352
Bowman J. D. et al., 2013, PASA, 30, 31
Christensen U. R., Aubert J., 2006, Geophys. J. Int., 166, 97
Christensen U. R., Holzwarth V., Reiners A., 2009, Nature, 457, 167
Condon J. J., Cotton W. D., Greisen E. W., Yin Q. F., Perley R. A., Taylor G. B., Broderick J. J., 1998, AJ, 115, 1693
Connerney J. E. P., 1993, J. Geophys. Res., 98, 18659
De Breuck C., Tang Y., de Bruyn A. G., Röttgering H., van Breugel W., 2002, A&A, 394, 59
Dulk G. A., 1985, ARA&A, 23, 169
Farrell W. M., Desch M. D., Zarka P., 1999, J. Geophys. Res., 104, 14025
George S. J., Stevens I. R., 2007, MNRAS, 382, 455
Grießmeier J.-M., Zarka P., Spreeuw H., 2007, A&A, 475, 359
Grießmeier J.-M., Zarka P., Girard J. N., 2011, Radio Sci., 46, 0
Hallinan G., Sirothia S. K., Antonova A., Ishwara-Chandra C. H., Bourke S., Doyle J. G., Hartman J., Golden A., 2013, ApJ, 762, 34
Hess S. L. G., Zarka P., 2011, A&A, 531, A29
Hurley-Walker N. et al., 2014, PASA, in press
Lazio W. T. J., Farrell W. M., Dietrick J., Greenlees E., Hogan E., Jones C., Hennig L. A., 2004, ApJ, 612, 511
Lazio J. et al., 2009, Astro2010: The Astronomy and Astrophysics Decadal Survey, Science White Papers, no. 177, Magnetospheric Emissions from Extrasolar Planets
Lazio T. J. W., Shankland P. D., Farrell W. M., Blank D. L., 2010, AJ, 140, 1929
Lecavelier des Etangs A., Sirothia S. K., Gopal-Krishna, Zarka P., 2013, A&A, 552, A65
Lonsdale C. J. et al., 2009, IEEE Proc., 97, 1497
Mayor M., Queloz D., 1995, Nature, 378, 355
Nichols J. D., 2012, MNRAS, 427, L75
Offringa A. R., van de Gronde J. J., Roerdink J. B. T. M., 2012, A&A, 539, A95
Offringa A. R. et al., 2014, MNRAS, 444, 606
Perryman M., 2011, The Exoplanet Handbook. Cambridge Univ. Press, Cambridge, UK
Schneider J. et al., 2011, A&A, 532, A79
Sirothia S. K., Lecavelier des Etangs A., Gopal-Krishna Kantharia N. G., Ishwar-Chandra C. H., 2014, A&A, 562, A108
Smith A. M. S., Collier Cameron A., Greaves J., Jardine M., Langston G., Backer D., 2009, MNRAS, 395, 335
Stroe A., Snellen I. A. G., Röttgering H. J. A., 2012, A&A, 546, A116
Tingay S. J. et al., 2013, PASA, 30, 7
van Leeuwen F., 2007, A&A, 474, 653
Winglee R. M., Dulk G. A., Bastian T. S., 1986, ApJ, 309, L59
Zarka P., Treumann R. A., Ryabov B. P., Ryabov V. B., 2001, Ap&SS, 277, 293
Zarka P., Cecconi B., Kurth W. S., 2004, J. Geophys. Res., 109, 9
Zarka P., Griessmeier J.-M., Tkp-ExoPlanets Working Group 2009, in Arabelos D. N., Tscherning C. C., eds, EGU General Assembly Conference Abstracts, LOFAR observations of Solar System planets and Exoplanets. European Geosciences Union, Vienna, p. 8776

This paper has been typeset from a TEX/LATEX file prepared by the author.